



Curvature effects on boundary migration

Claude Fressengeas

► To cite this version:

Claude Fressengeas. Curvature effects on boundary migration. Journal of the Mechanics and Physics of Solids, 2019, 124, pp.814-826. 10.1016/j.jmps.2018.11.024 . hal-02906263

HAL Id: hal-02906263

<https://hal.univ-lorraine.fr/hal-02906263>

Submitted on 24 Jul 2020

HAL is a multi-disciplinary open access archive for the deposit and dissemination of scientific research documents, whether they are published or not. The documents may come from teaching and research institutions in France or abroad, or from public or private research centers.

L'archive ouverte pluridisciplinaire **HAL**, est destinée au dépôt et à la diffusion de documents scientifiques de niveau recherche, publiés ou non, émanant des établissements d'enseignement et de recherche français ou étrangers, des laboratoires publics ou privés.

Curvature effects on boundary migration

Claude Fressengeas

Laboratoire d'Etude des Microstructures et de Mécanique des Matériaux
LEM3, Université de Lorraine/CNRS/Arts et Métiers ParisTech
7 rue Félix Savart, 57070 Metz, France

November 30, 2018

Abstract

We investigate continuity constraints on the plastic distortion and distortion rate tensors across surfaces of discontinuity moving through elastoplastic bodies. Tangential continuity of these tensors across interfaces moving normally to themselves derive from the conservation of the Burgers vector over patches bridging the interface, in the limit where such patches shrink onto the interface. Along interfaces whose motion involves a rotation, Burgers vector conservation follows from a trade-off between any tangential discontinuity of the dislocation-mediated plastic distortion rate relative to the interface and a plastic distortion rate arising from the rotation of the interface. The interface rotation dynamics follows from this balance. Additionally using the thermodynamic requirement of positive interface dissipation allows formulating mobility laws for the motion of the interface. The simplest admissible constitutive relationship relates the interface velocity to the traction vector. This mobility relationship recovers and develops in a tensorial context the conventional relations for grain boundary migration and grain growth in recovery/dynamic recrystallization processes, but challenges the constitutive character of the mobility parameter.

1 Introduction

The migration of grain boundaries (GBs) and the subsequent grain shape/grain size changes in the course of loading have long been seen as major mechanisms in the recovery and dynamic recrystallization of polycrystalline materials [Humphreys-Hatherly,1995]. GB migration has also been found relevant in the plasticity of nanocrystalline materials, where dislocation glide is limited by grain size [Sutton-Balluffi,1995; Cahn-Taylor,2004;

Cahn et al.,2006; Farkas,2006; Gianola et al.,2006; Momprou et al.,2009; Tucker et al.,2010; Momprou et al.,2011], or in materials lacking the independent slip systems needed to accommodate arbitrary external loading through dislocation motion, such as olivine in the Earth upper mantle [Cordier,2014].

Modeling efforts aimed at describing GB motion include surface-dislocation approaches. In the latter, surface-dislocations are defects singularly supported by interfaces, and designed to accommodate tangential discontinuities of the elastic distortion across the interface [Frank,1950; Bilby,1955]. Such approaches can be successful in predicting geometrical properties of grain boundaries, such as the coupling factor relating the normal motion of a tilt boundary to an imposed shear displacement [Cahn et al.,2006; Berbenni et al.,2013]. They may be taken more or less literally in certain circumstances: electron microscopy has revealed that the structure of low angle boundaries or semi-coherent interfaces actually involves dislocations [Priester,1979; Csiszár,2011]. In most cases however, the so-called surface-dislocations cannot be identified with observable dislocations and reduce to being only mathematical artefacts. For example, they do not represent the actual structure of high angle boundaries, because their spacing would have to be so small that their cores would overlap [Li,1972; Priester,2013]. As a result, surface-dislocation-based modeling approaches fail to account for the structure and energy of high-angle boundaries, because they overlook their core properties. Further, by allowing the accommodation of any tangential discontinuity of the elastic/plastic distortion and distortion rate across boundaries, they tend to reduce grain-to-grain interactions, with foreseeable consequences on the prediction of texture evolution and plastic strain localization [Mach et al.,2010; Taupin et al.,2016].

Atomistic simulations [Cahn et al.,2006; Farkas,2006; Tucker et al.,2010] and continuous descriptions based on crystal defect fields such as disclination dipoles [Cordier,2014; Fressengeas et al.,2014; Taupin et al.,2014; Sun et al.,2016] provide alternative approaches where the GB core structure and migration under applied stress can be thoroughly described at a resolution length scale of the order of inter-atomic spacing. In the present paper however, we have in mind a mesoscale representation where the spatial resolution length scale is not sufficiently small to reveal the core structure of the grain boundaries, but allows instead encompassing large polycrystals at relatively low cost. As in the surface-dislocation approaches, we see GBs as interfaces of vanishingly small thickness, across which the stress, total distortion, elastic/plastic distortion and distortion rate components may experience a discontinuity. Following [Acharya,2007; Fressengeas et al.,2012], we contend however that all such discontinuities are not acceptable. Besides tangential continuity of the total distortion/distortion rate tensor - the so-called Hadamard compatibility conditions [Hadamard,1903], which ensure continuity of the body across the interface, and normal continuity of the stress tensor (the traction vector needs to be continuous across the interface to respect mechanical equilibrium), we impose the conservation of the Burgers vector across the interface by removing any surface-dislocation density from the interface. Such a requirement induces non-locality of the elasto-plastic

response of the polycrystal across the interface, because elastic/plastic distortion values from the left of the interface have to be related to their counterparts from the right. Further, it amounts to distributing the dislocation density accumulating at grain boundaries over a finite volumetric boundary layer, perhaps of a small thickness - but definitely not vanishingly small. Such non-locality was shown to have a strong impact on the elastic/plastic strain and rotation fields in the vicinity of grain boundaries. It allowed retrieving such complex features as size and morphology effects, loading path-dependency, the Bauschinger effect and directional hardening in the plastic response of particle-reinforced alloys and thin polycrystalline films [Richeton,2011; Puri,2011], overall texture intensity and a β fiber more consistent with experimental observation in f.c.c. metals than the Taylor models [Mach et al.,2010], and shear strain localization in lamellar Al-Cu-Li alloys that conventional crystal plasticity fails to capture [Taupin et al.,2016].

Boundary curvature has long been known to determine grain growth. It is usually expected in recovery/recrystallization processes that the normal velocity C_n of a boundary moving into the parent crystal be given by the mobility relationship

$$C_n = M(p - p_d) \quad (1)$$

between the velocity and a driving force [Humphreys-Hatherly,1995]. In this relation, M is a constitutive mobility parameter, $p = \Delta E/L$ and $p_d = 2\gamma/R$ are driving pressures arising respectively from the jump in stored energy ΔE between the parent and recovered/recrystallized crystals of characteristic dimension L , and from the elastic surface energy γ of the boundary. The dependence on the mean curvature $1/R$ of the boundary derives from the elastic surface energy, assumed to be isotropic. The underlying mechanism for grain growth is assumed to be the elastically-driven thermally-activated transfer of atoms across the interface from one grain to the other, through grain boundary self-diffusion [Smoluchowski,1951; Burke-Turnbull,1952]. However, since the temperature dependence of grain growth has been observed to be different from that of surface energy in several materials [Allen-Cahn,1979], it has been suggested that this mechanism cannot be universal. Precipitate pinning may also be relevant in certain materials.

In the present paper, a dislocation-based mechanism is proposed for the interpretation of curvature effects on GB migration. In essence, the foreseeable relationships between the tangential jumps of the plastic distortion and distortion rate tensors across interfaces and the rotation dynamics of these interfaces are explored through Burgers vector conservation requirements. It is our aim to present on this basis thermo-mechanical modeling of curved interfaces moving through the material, having orientation (tensorial) character and with potential application to recovery and dynamic recrystallization. Grounded in the mechanical theory of continuously distributed dislocations [Kröner,1981; Acharya,2001], the model extends the tangential continuity requirements [Acharya,2007] to interfaces featuring curvature dynamics, and explores the thermodynamic constraints on interface motion eventually arising from positiveness of the mechanical dissipation. The outline

of the paper is therefore as follows. After setting up notations in Section 2, a review of the tangential continuity conditions on the plastic/total distortion/distortion rate tensors across interfaces propagating normally to themselves is provided in Section 3. Section 4 presents the Burgers vector conservation constraints pertaining to curved interfaces encountering rotation rates and the resulting curvature dynamics. Section 5 provides the driving force and admissible mobility laws emerging from the thermodynamic requirement of positive mechanical dissipation at interfaces. Conclusions on the potential applicability of the analysis to recrystallization/recovery phenomena and to the plasticity of ultrafine-grained materials follow.

2 Notations

A bold symbol denotes a tensor, as in: \mathbf{A} . When there may be ambiguity, an arrow is superposed to represent a vector: $\vec{\mathbf{V}}$. The transpose of tensor \mathbf{A} is \mathbf{A}^t . All tensor subscript indices are written with respect to the basis $(\mathbf{e}_i, i = 1, 2, 3)$ of a rectangular Cartesian coordinate system. Vertical arrays of one or two dots represent contraction of the respective number of "adjacent" indices on two immediately neighboring tensors, in standard fashion. For example, the tensor $\mathbf{A} \cdot \mathbf{B}$ with components $A_{ik}B_{kj}$ results from the dot product of tensors \mathbf{A} and \mathbf{B} , and $\mathbf{A} : \mathbf{B} = A_{ij}B_{ij}$ represents their inner product. The cross product of a second order tensor \mathbf{A} and a vector \mathbf{V} , the **div** and **curl** operations for second order tensors are defined row by row, in analogy with the vectorial case. For example:

$$(\mathbf{A} \times \mathbf{V})_{ij} = e_{jkl}A_{ik}V_l \quad (2)$$

$$(\mathbf{div} \mathbf{A})_i = A_{ij,j} \quad (3)$$

$$(\mathbf{curl} \mathbf{A})_{ij} = e_{jkl}A_{il,k}. \quad (4)$$

where $e_{jkl} = \mathbf{e}_j \cdot (\mathbf{e}_k \times \mathbf{e}_l)$ is a component of the third-order alternating Levi-Civita tensor \mathbf{X} , equal to 1 if the jkl permutation is even, -1 if it is odd and 0 otherwise. In the component representation, the comma followed by a component index indicates a spatial derivative with respect to the corresponding Cartesian coordinate as in relations (3,4). A vector $\vec{\mathbf{A}}$ is associated with tensor \mathbf{A} by using the inner product of \mathbf{A} with tensor \mathbf{X} :

$$(\vec{\mathbf{A}})_k = -\frac{1}{2}(\mathbf{X} : \mathbf{A})_k = -\frac{1}{2}e_{kij}A_{ij} \quad (5)$$

$$(\mathbf{A})_{ij} = -(\mathbf{X} \cdot \vec{\mathbf{A}})_{ij} = -e_{ijk}(\vec{\mathbf{A}})_k. \quad (6)$$

The symmetric and skew-symmetric parts of tensor \mathbf{A} are denoted \mathbf{A}^{sym} and \mathbf{A}^{skew} respectively. Given a unit vector \mathbf{n} normal to an interface I in a domain D and orienting I from sub-domain D^- to sub-domain D^+ , the normal part \mathbf{A}_n and tangential part \mathbf{A}_t of

tensor \mathbf{A} are

$$\mathbf{A}_n = \mathbf{A} \cdot \mathbf{n} \otimes \mathbf{n} \quad (7)$$

$$\mathbf{A}_t = \mathbf{A} - \mathbf{A}_n. \quad (8)$$

For a vector \mathbf{V} :

$$\mathbf{V}_n = (\mathbf{V} \cdot \mathbf{n})\mathbf{n} = V_n \mathbf{n} \quad (9)$$

$$\mathbf{V}_t = \mathbf{V} - \mathbf{V}_n. \quad (10)$$

The discontinuity of a tensor \mathbf{A} at the interface I is denoted $\llbracket \mathbf{A} \rrbracket = \mathbf{A}^+ - \mathbf{A}^-$, where \mathbf{A}^- and \mathbf{A}^+ are the limits of tensor \mathbf{A} when evaluated at limit points on the interface along direction \mathbf{n} in D^- and D^+ , respectively. The average value across the interface is: $\langle \mathbf{A} \rangle = (\mathbf{A}^+ + \mathbf{A}^-)/2$. A superposed dot represents a material time derivative.

3 Tangential continuity constraints along moving interfaces

Material properties and/or field variables, such as the elastic/plastic displacement and distortion/distortion rate fields or the dislocation density field may encounter discontinuities across surfaces moving throughout the body, such as migrating grain boundaries or embryo-parent crystal interfaces in recrystallization phenomena. However, not all discontinuities are allowed: the continuity of matter and the conservation of the Burgers vector across such interfaces mandate satisfaction of partial continuity conditions. The constraints on the discontinuity of the total distortion across interfaces moving normally to themselves, also known as Hadamard's compatibility conditions [Hadamard,1903], are first reviewed. We assume the existence of a surface of discontinuity I separating the body \mathcal{B} into two sub-domains \mathcal{B}^- and \mathcal{B}^+ , and moving into \mathcal{B}^+ . At any point P on I , the unit normal vector \mathbf{n} to the interface is oriented from \mathcal{B}^- toward \mathcal{B}^+ , and we denote by \mathbf{l} and $\boldsymbol{\tau} = \mathbf{n} \times \mathbf{l}$ two unit vectors belonging to the interface (see Fig.1). In the absence of cracks and shocks, continuum mechanics respectively requires that the displacement \mathbf{u} and traction vector $\mathbf{t} = \mathbf{T} \cdot \mathbf{n}$ be continuous across the interface: $\llbracket \mathbf{u} \rrbracket = 0$, $\llbracket \mathbf{t} \rrbracket = 0$. The continuity of the traction vector is reflected as well by the continuity of the normal part, $\mathbf{T}_n = \mathbf{T} \cdot \mathbf{n} \otimes \mathbf{n}$, of the stress tensor: $\llbracket \mathbf{T}_n \rrbracket = 0$, whereas the tangential part $\mathbf{T}_t = \mathbf{T} - \mathbf{T}_n$ of the latter may be discontinuous across the interface. Continuity of the displacement at the interface requires that the total distortion \mathbf{U} be a gradient tensor and therefore satisfy

$$\int_C \mathbf{U} \cdot d\mathbf{x} = 0 \quad (11)$$

along the rectangular closed circuit C lying across the interface as shown in Fig.1. When C is collapsed onto point P by letting $L \rightarrow 0$, $h^- \rightarrow 0$, $h^+ \rightarrow 0$, the limit of the above

integral provides

$$\forall \mathbf{l} \in I, \llbracket \mathbf{U} \rrbracket \cdot \mathbf{l} = 0, \quad (12)$$

a relation whose meaning is tangential continuity of the total distortion. This property is also rendered more compactly as:

$$\llbracket \mathbf{U} \rrbracket \times \mathbf{n} = 0, \quad (13)$$

or as $\llbracket \mathbf{U} \rrbracket_t = 0$. The discontinuity of the distortion is therefore limited to its normal part $\llbracket \mathbf{U} \rrbracket_n$. The total displacement derivative at points moving with the interface is given by the kinematic relation

$$\frac{d\mathbf{u}}{dt} = \mathbf{v} + \mathbf{U} \cdot \mathbf{C}, \quad (14)$$

where \mathbf{v} is the material velocity and $\mathbf{C} = C_n \mathbf{n}$ the velocity of the interface with respect to the material in direction \mathbf{n} . Continuity of the displacement across the interface therefore implies that the discontinuity $\llbracket \mathbf{U} \rrbracket$ of the distortion relates to the discontinuity of the velocity $\llbracket \mathbf{v} \rrbracket$ through the relation:

$$\llbracket \mathbf{v} \rrbracket + \llbracket \mathbf{U} \rrbracket \cdot \mathbf{C} = 0. \quad (15)$$

Performing the dyadic product of each term in this relation with the normal \mathbf{n} , we find

$$\llbracket \mathbf{v} \rrbracket \otimes \mathbf{n} + \llbracket \mathbf{U} \rrbracket \cdot \mathbf{C} \otimes \mathbf{n} = 0, \quad (16)$$

which leads to

$$\llbracket \mathbf{U} \rrbracket = \llbracket \mathbf{U} \rrbracket_n = -\frac{1}{C_n} \llbracket \mathbf{v} \rrbracket \otimes \mathbf{n}. \quad (17)$$

By differentiating Eq.11 with respect to time, tangential continuity is also found to apply to the total distortion rate $\dot{\mathbf{U}}$:

$$\forall \mathbf{l} \in I, \llbracket \dot{\mathbf{U}} \rrbracket \cdot \mathbf{l} = 0 \quad (18)$$

$$\llbracket \dot{\mathbf{U}} \rrbracket \times \mathbf{n} = 0, \quad (19)$$

whereas the normal part $\dot{\mathbf{U}}_n$ of the distortion rate tensor may encounter a discontinuity. Of course, the satisfaction of relations (13,15,17,19) precludes any occurrence of matter disruption mechanisms at interfaces, such as grain boundary sliding or cavitation. However, Hadamard's compatibility equations (13,15,17) do not impose any constraint on the plastic distortion tensor \mathbf{U}_p at the interface. We show below that tangential continuity conditions on \mathbf{U}_p arise at the interface if the choice is made to represent continuously the dislocations in the interface area by adopting a small resolution length scale [Acharya,2007].

In this aim, we consider again the rectangular closed circuit C lying across the interface, as well as two sub-circuits C^- and C^+ defined in the manner shown in Fig.1. The

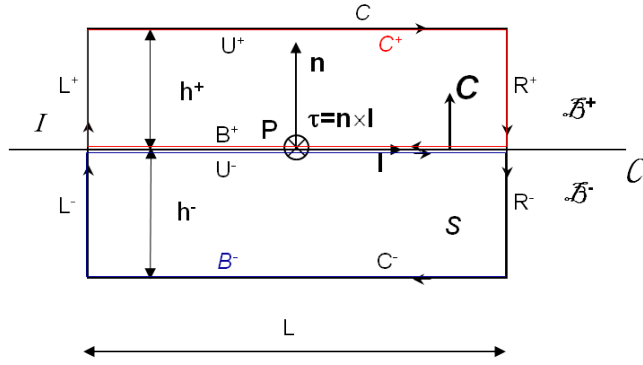


Figure 1: Burgers circuit $C = U^+ \cup R^+ \cup R^- \cup B^- \cup L^- \cup L^+$ across an interface I separating the body \mathcal{B} into domains \mathcal{B}^- , \mathcal{B}^+ . \mathbf{l} is the unit tangent to curve \mathcal{C} , \mathbf{n} is the unit normal to interface I , and $\boldsymbol{\tau} = \mathbf{n} \times \mathbf{l}$ the "tangent normal" to the bounded surface S and curve \mathcal{C} . Two distinct sub-circuits $C^- = U^- \cup R^- \cup B^- \cup L^-$ and $C^+ = U^+ \cup R^+ \cup B^+ \cup L^+$ belong to \mathcal{B}^- and \mathcal{B}^+ . $\mathbf{C} = C\mathbf{n}$ is the velocity of the interface with respect to the body.

intersection of surface S and interface I defines a curve \mathcal{C} on I , to which the orthonormal frame $\mathcal{D} = (P, \mathbf{e}_1 = \mathbf{l}, \mathbf{e}_2 = \boldsymbol{\tau}, \mathbf{e}_3 = \mathbf{n})$ is a natural moving frame at point P . \mathcal{D} is referred to as the Darboux frame of curve \mathcal{C} on I (see Fig.2) [Darboux,1888]. The frame \mathcal{D} is simply translated in the normal motion of the interface. A bulk dislocation density field $\boldsymbol{\alpha}$ is assumed to take place over surface S , and a surface-dislocation density $\boldsymbol{\alpha}^S(I)$ is provisionally allowed to exist along the interface I . To first comment on the role of the surface-dislocation density $\boldsymbol{\alpha}^S(I)$, we consider the limit of the Burgers vector content of circuit C

$$\mathbf{b} = - \int_C \mathbf{U}_p \cdot \mathbf{l} ds = \int_S \boldsymbol{\alpha} \cdot \boldsymbol{\tau} dS. \quad (20)$$

when C is collapsed onto point P by letting $L \rightarrow 0, h^- \rightarrow 0, h^+ \rightarrow 0$ as previously. We find:

$$\forall \mathbf{l} \in I, -\llbracket \mathbf{U}_p \rrbracket \cdot \mathbf{l} = \boldsymbol{\alpha}^S(I) \cdot \boldsymbol{\tau}. \quad (21)$$

This relation is nothing else than the celebrated Frank's relation of the theory of dislocations [Frank,1950; Bilby,1955], which provides

$$\boldsymbol{\alpha}^S(I) = \llbracket \mathbf{U}_p \rrbracket \times \mathbf{n}. \quad (22)$$

Its meaning is that, whatever the tangential discontinuity $\llbracket \mathbf{U}_p \rrbracket$ of the plastic distortion, it can be accommodated by an appropriate surface-dislocation density tensor $\boldsymbol{\alpha}^S(I)$. It must be borne in mind that $\boldsymbol{\alpha}^S(I)$ and the dislocation density tensor $\boldsymbol{\alpha}$ are mathematical objects of a different nature. Whereas $\boldsymbol{\alpha}$ (expressed in units of Burgers vector length per unit surface) is a continuously defined field representing a volumetric dislocation ensemble in the bulk of the material, $\boldsymbol{\alpha}^S(I)$ (in units of Burgers vector length per unit length, *i.e.* non dimensional) is a surfacic density field supported by the singular interface I . As indicated in the introduction Section, these surface-dislocations cannot in general be identified with observable dislocations. They usually reduce to being only mathematical artefacts whose role is, as indicated above, to accommodate a tangential discontinuity of the plastic distortion across the interface. In order to restore tangential continuity of the plastic distortion, we shall instead assume $\boldsymbol{\alpha}^S(I) = 0$ in the following. Thus, we set the condition

$$\forall \mathbf{l} \in I, \llbracket \mathbf{U}_p \rrbracket \cdot \mathbf{l} = 0. \quad (23)$$

A more compact way of stating this property is alternatively:

$$\llbracket \mathbf{U}_p \rrbracket \times \mathbf{n} = 0, \quad (24)$$

or $\llbracket \mathbf{U}_p \rrbracket_t = 0$. The effect of such a constraint is to distribute the dislocation density arising from plastic distortion incompatibility at the interface over a finite volumetric boundary layer, perhaps of a small thickness - but definitely not vanishingly small. In doing so, nonlocal interactions between domains \mathcal{B}^- and \mathcal{B}^+ across the interface are promoted, because values of the plastic distortion at different points on either sides of the

interface have to be equal. Of course, Eqs.(23,24) are silent about the normal discontinuity $[[\mathbf{U}_p]]_n$, which involves a plastic shear jump with components in the local frame \mathcal{D} ($[[\epsilon_{13}^p]] = [[\epsilon_{31}^p]]$, $[[\epsilon_{23}^p]] = [[\epsilon_{32}^p]]$), a normal stretch jump $[[\epsilon_{33}^p]]$ and a tilt rotation vector jump ($[[\omega_1^p]]$, $[[\omega_2^p]]$) and can very well be non-zero. However, compatibility conditions between these normal discontinuities arise when several interfaces with respective discontinuities of the plastic distortions $[[\mathbf{U}_p]]_i$, $i \in (1, 2, \dots, N)$ connect along a multiple-line, in practice a triple-line with $N = 3$ in polycrystals. Indeed, closure requires that the sum of all discontinuities vanish at the multiple-line:

$$\sum_{i=1}^N [[\mathbf{U}_p]]_i = 0 \quad (25)$$

because the same grain is used to start and finish a closed circuit around the multiple-line. Summing the relations (24) for all interfaces, and using Eq.25, it is seen that the normal discontinuities in the plastic distortion need to satisfy a Kirchhoff-type relation at the multiple-line:

$$\sum_{i=1}^N [[\mathbf{U}_p]]_i \cdot \mathbf{n}_i \otimes \mathbf{n}_i = 0. \quad (26)$$

When all normals \mathbf{n}_i are coplanar, Eq.26 reduces to an Herring-type relationship at the multiple-line [Fressengeas et al.,2012].

Now, writing the plastic distortion rate tensor as: $\dot{\mathbf{U}}_p = \boldsymbol{\alpha} \times \mathbf{V}$ where \mathbf{V} is the dislocation velocity with respect to the material, and performing the time-derivative of the net Burgers vector obtained from the circuit C^+ in Eq.20, collapsing C^+ onto point $P \in I$ by letting again $L \rightarrow 0$, $h^- \rightarrow 0$, $h^+ \rightarrow 0$, we obtain

$$\forall \mathbf{l} \in I, \boldsymbol{\alpha}^+ \times (\mathbf{V}^+ - \mathbf{C}).\mathbf{l} = 0. \quad (27)$$

Similarly, the circuit C^- leads to the relation

$$\forall \mathbf{l} \in I, -\boldsymbol{\alpha}^- \times (\mathbf{V}^- - \mathbf{C}).\mathbf{l} = 0. \quad (28)$$

Combining the obtained relations yields the jump condition

$$\forall \mathbf{l} \in I, [[\boldsymbol{\alpha} \times (\mathbf{V} - \mathbf{C})]].\mathbf{l} = 0, \quad (29)$$

which reflects Burgers vector conservation at the moving interface [Acharya,2007] and may alternatively read in compact form:

$$[[\boldsymbol{\alpha} \times (\mathbf{V} - \mathbf{C})]] \times \mathbf{n} = 0. \quad (30)$$

The dislocations implied in Eq.30 on both sides \mathcal{B}^- and \mathcal{B}^+ will be referred to in the following as "interfacial dislocations". From the above developments, it should be clear

that they are defined on volume elements and are not surface-dislocations. Their velocity with respect to the material can be decomposed on both sides of the interface into normal $\mathbf{V}_n = V_n \mathbf{n}$ and tangential \mathbf{V}_t components, such that $\mathbf{V} = \mathbf{V}_n + \mathbf{V}_t$. Eq.30 reads in component form in the Darboux frame:

$$\llbracket e_{jkl} e_{krs} \alpha_{ir} (V_s - C_s) n_l \rrbracket = \llbracket \alpha_{il} (V_j - C_j) n_l - \alpha_{ij} (V_l - C_l) n_l \rrbracket = 0. \quad (31)$$

The extreme-right equality in Eq.31 is equivalently, in intrinsic form:

$$\llbracket \boldsymbol{\alpha} \cdot \mathbf{n} \otimes \mathbf{V}_t - (V_n - C_n) \boldsymbol{\alpha}_t \rrbracket = 0, \quad (32)$$

where $\boldsymbol{\alpha}_t$ is the tangential part of $\boldsymbol{\alpha}$, *i.e.* the part reflecting dislocation lines parallel to the interface, such that $\boldsymbol{\alpha}_t \cdot \mathbf{n} = 0$ (see Eqs.(7,8)). From Eq.32, it is seen that $\boldsymbol{\alpha}_t$ satisfies Burgers vector conservation when $V_n = C_n$, *i.e.* when the corresponding dislocations follow the interface in its motion, possibly with a tangential velocity \mathbf{V}_t . It is also apparent from Eq.32 and from the identity

$$\llbracket \boldsymbol{\alpha} \cdot \mathbf{n} \otimes \mathbf{V}_t \rrbracket = \llbracket \boldsymbol{\alpha} \cdot \mathbf{n} \rrbracket \otimes \langle \mathbf{V}_t \rangle + \langle \boldsymbol{\alpha} \cdot \mathbf{n} \rangle \otimes \llbracket \mathbf{V}_t \rrbracket \quad (33)$$

that the normal part $\boldsymbol{\alpha}_n$ of $\boldsymbol{\alpha}$, which reflects dislocation lines normal to the interface ($\boldsymbol{\alpha} \cdot \mathbf{n} \neq 0$ and $\boldsymbol{\alpha}_t = 0$), satisfies Burgers vector conservation either when $\llbracket \boldsymbol{\alpha} \cdot \mathbf{n} \rrbracket = 0$ and $\llbracket \mathbf{V}_t \rrbracket = 0$, or if $\llbracket \boldsymbol{\alpha} \cdot \mathbf{n} \rrbracket \neq 0$ when $\mathbf{V}_t = 0$ on both sides of the interface.

4 Curvature effects on tangential continuity constraints

Interfaces moving faster than dislocations lying ahead, and therefore such that $V_n \neq C_n$, are commonplace in recrystallization phenomena. Hence, the existence of tangential interfacial dislocations ($\boldsymbol{\alpha}_t \neq 0$) leading to the violation of Eq.30 is likely. Further, interfacial dislocations moving along the interface ($\mathbf{V}_t \neq 0$) have been reported in *Al* bi-crystals [Kegg et al.,1973; Mori-Tangri,1979; Momprou et al.,2013], even at low temperatures and small strains. Among the latter, dislocations belonging to the normal part of $\boldsymbol{\alpha}$ ($\boldsymbol{\alpha} \cdot \mathbf{n} \neq 0$) and gliding along the interface were evidenced on one side of the interface in [Mori-Tangri,1979], implying $\llbracket \boldsymbol{\alpha} \cdot \mathbf{n} \rrbracket \neq 0$ and $\llbracket \mathbf{V}_t \rrbracket \neq 0$ so that Eq.30 was not satisfied. To account for such apparent violations of the Burgers vector conservation constraint, we now revisit this condition along a moving interface I by complementarily accounting for possible rotations of the Darboux frame along the moving curves \mathcal{C} . We consider again the closed circuit C bounding surface S , and the sub-circuits C^- and C^+ shown in Fig.1, but the Darboux frame \mathcal{D} of curves \mathcal{C} is now allowed to rotate in the motion of point P along the moving interface I , with the rotation rate $\dot{\boldsymbol{\Omega}}$:

$$\dot{\boldsymbol{\Omega}} = \left(-\frac{1}{T} + \frac{\boldsymbol{\tau}}{R_n} + \frac{\mathbf{n}}{R_g} \right) \dot{s}. \quad (34)$$

In this relation, (T, R_n, R_g) are respectively the geodesic torsion, normal and geodesic curvature radii of curve \mathcal{C} on interface I , and s is the arc length along curve \mathcal{C} (see Fig.2). Further, the time-derivatives of the Darboux unit vectors are [Darboux,1888; Cartan,1937]

$$\dot{\mathbf{e}}_i = \dot{\boldsymbol{\Omega}} \times \mathbf{e}_i. \quad (35)$$

Thus, performing again the time-derivative of the integral (11) and collapsing C to point P by letting $L \rightarrow 0, h^- \rightarrow 0, h^+ \rightarrow 0$, we now obtain

$$\forall \mathbf{l} \in I, \llbracket \dot{\mathbf{U}} \rrbracket \cdot \mathbf{l} + \llbracket \mathbf{U} \rrbracket \cdot \dot{\mathbf{l}} = 0, \quad (36)$$

and hence successively, using Eq.35:

$$\forall \mathbf{l} \in I, \llbracket \dot{\mathbf{U}} \rrbracket \cdot \mathbf{l} + \llbracket \mathbf{U} \rrbracket \cdot \dot{\boldsymbol{\Omega}} \times \mathbf{l} = 0 \quad (37)$$

$$\forall \mathbf{l} \in I, (\llbracket \dot{\mathbf{U}} \rrbracket + \llbracket \mathbf{U} \rrbracket \times \dot{\boldsymbol{\Omega}}) \cdot \mathbf{l} = 0 \quad (38)$$

$$(\llbracket \dot{\mathbf{U}} \rrbracket + \llbracket \mathbf{U} \rrbracket \times \dot{\boldsymbol{\Omega}}) \times \mathbf{n} = 0. \quad (39)$$

Using the vector triple product expansion for the last term (also used in component form in Eq.31 above), we find:

$$\llbracket \dot{\mathbf{U}} \rrbracket \times \mathbf{n} + \llbracket \mathbf{U} \rrbracket \cdot \mathbf{n} \otimes \dot{\boldsymbol{\Omega}}_t - (\dot{\boldsymbol{\Omega}} \cdot \mathbf{n}) \cdot \llbracket \mathbf{U} \rrbracket_t = 0, \quad (40)$$

and finally, since $\llbracket \mathbf{U} \rrbracket_t = 0$ according to Eq.13

$$\llbracket \dot{\mathbf{U}} \rrbracket \times \mathbf{n} + \llbracket \mathbf{U} \rrbracket \cdot \mathbf{n} \otimes \dot{\boldsymbol{\Omega}}_t = 0, \quad (41)$$

where $\dot{\boldsymbol{\Omega}}_t$ is the tangential part of the rotation rate, involving only geodesic torsion and normal curvature. Eq.41 modifies the constraint (19) on the distortion rate jump across the interface when the rotation of Darboux frame needs to be accounted. However, continuity of matter is maintained because any tangential discontinuity of the plastic distortion rate is offset by the rotation of the interface, and Hadamard's compatibility conditions (13,17) on the discontinuity of the normal distortion are left unaffected. Matter disruption produced for instance by grain boundary sliding or crack nucleation in the vicinity of triple lines may occur in practice, but is not considered in the present analysis.

Performing again the time-derivative of the net Burgers vector for the circuits (C^-, C^+) in Eq.20, collapsing (C^-, C^+) onto the point P of the interface I by letting $L \rightarrow 0, h^- \rightarrow 0, h^+ \rightarrow 0$, and subtracting the resulting relations, we also obtain:

$$\forall \mathbf{l} \in I, \llbracket \boldsymbol{\alpha} \times (\mathbf{V} - \mathbf{C}) \rrbracket \cdot \mathbf{l} + \llbracket \mathbf{U}_p \rrbracket \cdot \dot{\mathbf{l}} = 0 \quad (42)$$

if surface-dislocations are not allowed to take place along I . Using Eq.35, this relation becomes:

$$\forall \mathbf{l} \in I, \llbracket \boldsymbol{\alpha} \times (\mathbf{V} - \mathbf{C}) \rrbracket \cdot \mathbf{l} + \llbracket \mathbf{U}_p \rrbracket \cdot (\dot{\boldsymbol{\Omega}} \times \mathbf{l}) = 0, \quad (43)$$

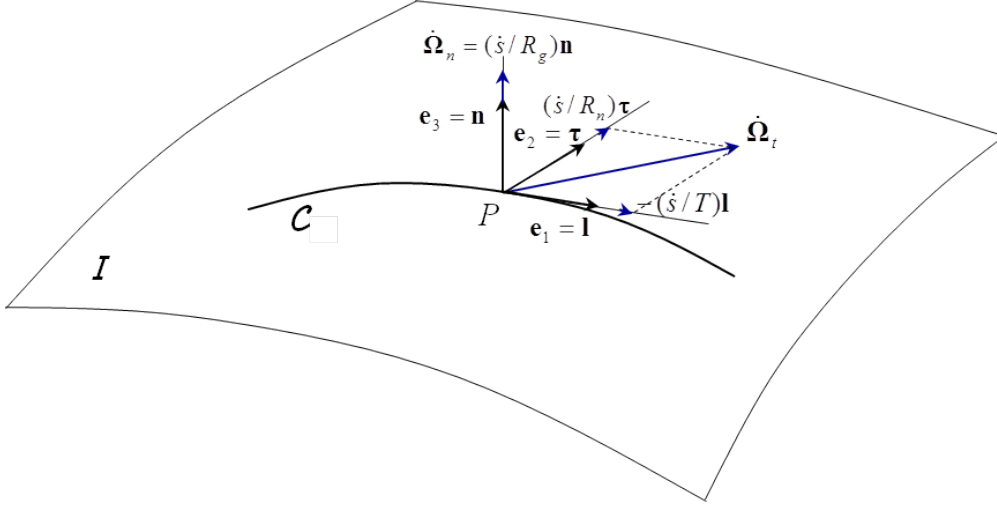


Figure 2: Darboux frame $(\mathbf{l}, \boldsymbol{\tau}, \mathbf{n}) = (\mathbf{e}_1, \mathbf{e}_2, \mathbf{e}_3)$ of curve \mathcal{C} on interface I and its rotation rate $\dot{\boldsymbol{\Omega}} = \dot{\boldsymbol{\Omega}}_n + \dot{\boldsymbol{\Omega}}_t$

and successively

$$\forall \mathbf{l} \in I, \llbracket \boldsymbol{\alpha} \times (\mathbf{V} - \mathbf{C}) \rrbracket \cdot \mathbf{l} + (\llbracket \mathbf{U}_p \rrbracket \times \dot{\boldsymbol{\Omega}}) \cdot \mathbf{l} = 0 \quad (44)$$

$$\forall \mathbf{l} \in I, (\llbracket \boldsymbol{\alpha} \times (\mathbf{V} - \mathbf{C}) \rrbracket + \llbracket \mathbf{U}_p \rrbracket \times \dot{\boldsymbol{\Omega}}) \cdot \mathbf{l} = 0 \quad (45)$$

$$(\llbracket \boldsymbol{\alpha} \times (\mathbf{V} - \mathbf{C}) \rrbracket + \llbracket \mathbf{U}_p \rrbracket \times \dot{\boldsymbol{\Omega}}) \times \mathbf{n} = 0. \quad (46)$$

In the manner of Eq.40, we may also transform Eq.46 into:

$$\llbracket \boldsymbol{\alpha} \times (\mathbf{V} - \mathbf{C}) \rrbracket \times \mathbf{n} + \llbracket \mathbf{U}_p \rrbracket \cdot \mathbf{n} \otimes \dot{\boldsymbol{\Omega}}_t - \dot{\boldsymbol{\Omega}}_n \llbracket \mathbf{U}_p \rrbracket_t = 0. \quad (47)$$

Since $\llbracket \mathbf{U}_p \rrbracket_t = 0$ according to Eq.24, we find:

$$\llbracket \boldsymbol{\alpha} \times (\mathbf{V} - \mathbf{C}) \rrbracket \times \mathbf{n} + \llbracket \mathbf{U}_p \rrbracket \cdot \mathbf{n} \otimes \dot{\boldsymbol{\Omega}}_t = 0. \quad (48)$$

The interpretation of Eq.48 is that any tangential discontinuity of the relative plastic distortion rate $\boldsymbol{\alpha} \times (\mathbf{V} - \mathbf{C})$ can be offset by a complementary jump of a distortion rate originating in the tangential rotation of the interface, provided that a jump of the cumulated plastic distortion vector $\llbracket \mathbf{U}_p \rrbracket \cdot \mathbf{n}$ is already existing. As a result, overall conservation of the Burgers vector is ensured. Further, tangential continuity of the relative plastic distortion rate arising from the motion of the remaining dislocations still holds and consistency with the dislocation transport equation is retained¹ [Acharya,2007]. Of course,

¹It is perhaps worth noting that $\llbracket \mathbf{U}_p \rrbracket = \llbracket \mathbf{U}_p^\parallel + \mathbf{U}_p^\perp \rrbracket = \llbracket \mathbf{U}_p^\parallel - \mathbf{U}_e^\perp \rrbracket$. Thus, if the compatible plastic distortion \mathbf{U}_p^\parallel is, without loss of generality, arbitrarily set to zero at the time of interest, the jump of the plastic distortion reduces to $\llbracket \mathbf{U}_p \rrbracket = -\llbracket \mathbf{U}_e^\perp \rrbracket$, recalling that the jump of the incompatible elastic distortion associated with the presence of dislocations on either sides of the interface is fundamentally involved in the last brackets in Eqs.(46,48).

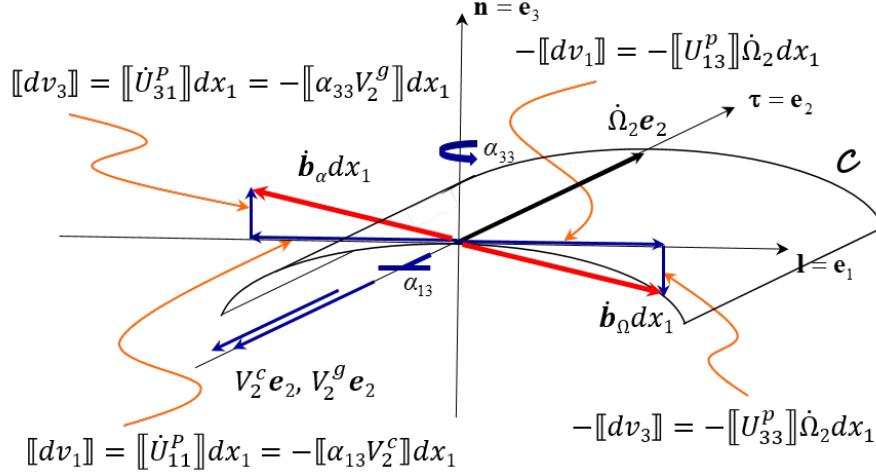


Figure 3: Tangential continuity trade-off across a cylindrical interface for the differential element $dx_1 \mathbf{e}_1$ along the principal tangential direction $\mathbf{l} = \mathbf{e}_1$ of curve C in the Darboux frame $(\mathbf{l}, \boldsymbol{\tau}, \mathbf{n}) = (\mathbf{e}_1, \mathbf{e}_2, \mathbf{e}_3)$. In the tangential direction \mathbf{e}_1 , the surface-dislocation nucleation rate $\dot{\mathbf{b}}_\alpha \cdot \mathbf{e}_1 = \llbracket \dot{U}_{11}^p \rrbracket$ and $\llbracket dv_1 \rrbracket$ velocity jump arising from the axial climb velocity $V_2^c \mathbf{e}_2$ of the edge dislocations α_{13} are offset by the surface-dislocation nucleation rate $\dot{\mathbf{b}}_\Omega \cdot \mathbf{e}_1 = -\llbracket \dot{U}_{11}^p \rrbracket$ and $-\llbracket dv_1 \rrbracket$ jump stemming from the shear jump $-\llbracket U_{13}^p \rrbracket$ acting on the velocity $dw_3 = \Omega_2 dx_1$. In the normal direction $\mathbf{n} = \mathbf{e}_3$, the nucleation rate $\dot{\mathbf{b}}_\alpha \cdot \mathbf{e}_3 = \llbracket \dot{U}_{31}^p \rrbracket$ and velocity jump $\llbracket dv_3 \rrbracket$ arising from the tangential glide velocity $V_2^g \mathbf{e}_2$ of the screw dislocations α_{33} are offset by the nucleation rate $\dot{\mathbf{b}}_\Omega \cdot \mathbf{e}_3$ and velocity jump $-\llbracket dv_3 \rrbracket$ stemming from the stretching jump $-\llbracket U_{33}^p \rrbracket$ acting on the velocity $dw_3 = \Omega_2 dx_1$. Thus: $\dot{\mathbf{b}}_\Omega + \dot{\mathbf{b}}_\alpha = 0$.

Eq.48 recovers our previous result: even in the presence of a normal plastic distortion jump $\llbracket \mathbf{U}_p \rrbracket \cdot \mathbf{n} \neq 0$, the tangential rotation rate $\dot{\boldsymbol{\Omega}}_t$ of the Darboux frame \mathcal{D} vanishes if $\llbracket \boldsymbol{\alpha} \times (\mathbf{V} - \mathbf{C}) \rrbracket \times \mathbf{n} = 0$. Restricting the developments to the normal part of the dislocation density tensor for the sake of simplicity and using Eqs.(31,32) in this aim, Eq.48 reads in component form in the Darboux frame:

$$\forall i \in \{1, 2, 3\}, \forall j \in \{1, 2\}, \llbracket \alpha_{i3} V_j \rrbracket + \llbracket U_{i3}^p \rrbracket \dot{\Omega}_j = 0, \quad (49)$$

or:

$$\frac{\llbracket \alpha_{13} V_1^g \rrbracket}{\llbracket U_{13}^p \rrbracket} = \frac{\llbracket \alpha_{23} V_1^c \rrbracket}{\llbracket U_{23}^p \rrbracket} = \frac{\llbracket \alpha_{33} V_1^g \rrbracket}{\llbracket U_{33}^p \rrbracket} = -\dot{\Omega}_1 \quad (50)$$

$$\frac{\llbracket \alpha_{13} V_2^c \rrbracket}{\llbracket U_{13}^p \rrbracket} = \frac{\llbracket \alpha_{23} V_2^g \rrbracket}{\llbracket U_{23}^p \rrbracket} = \frac{\llbracket \alpha_{33} V_2^g \rrbracket}{\llbracket U_{33}^p \rrbracket} = -\dot{\Omega}_2, \quad (51)$$

where the superscripts "g" and "c" of the dislocation velocities are for "glide" and "climb" respectively. Consider first for illustration the principal directions $(\mathbf{e}_1, \mathbf{e}_2)$ of a cylindrical

surface of axial direction \mathbf{e}_2 . Hence, the principal curvature $1/R_2$ vanishes, while the principal (normal) curvature $1/R_1$ is non-zero. Further, the surface torsion $1/T$ vanishes in the two principal directions. Assume consistently that interfacial dislocations $(\alpha_{13}, \alpha_{33})$ move in the axial direction \mathbf{e}_2 . Then $\dot{\Omega}_1 = 0, \dot{\Omega}_2 = \dot{s}/R_1 \neq 0$ and Eq.51 reduces to

$$\frac{[\![\alpha_{13}V_2^c]\!]}{[\![U_{13}^p]\!]} = \frac{[\![\alpha_{33}V_2^g]\!]}{[\![U_{33}^p]\!]} = -\dot{\Omega}_2. \quad (52)$$

In Eq.52, climb of the α_{13} edge dislocations in the axial direction \mathbf{e}_2 results in the stretching rate jump $[\![\dot{U}_{11}^p]\!] = -[\![\alpha_{13}V_2^c]\!]$ of a differential element dx_1 in the direction \mathbf{e}_1 . As sketched in Fig.3, this jump is offset by an opposite jump arising from the distortion jump $[\![U_{13}^p]\!]$ and axial rotation rate $\dot{\Omega}_2$ acting on dx_1 . Similarly, the distortion rate jump $[\![\dot{U}_{31}^p]\!] = -[\![\alpha_{33}V_2^g]\!]$ due to motion of the α_{33} screws in the axial direction is offset by an opposite jump arising from the stretching jump $[\![U_{33}^p]\!]$ and rotation rate $\dot{\Omega}_2$ acting on dx_1 (see Fig.3). As a result, normal curvature dynamics derives from the motion in the axial direction \mathbf{e}_2 of the interfacial dislocations $(\alpha_{13}, \alpha_{33})$.

As a second example, assume now that interfacial edge dislocations α_{13} glide with velocity V_1^g in the tangential direction \mathbf{e}_1 of a quasi-spherical interface (with two non-zero principal curvatures), thus inducing the stretching rate jump $[\![\dot{U}_{22}^p]\!] = [\![\alpha_{13}V_1^g]\!]$ of a tangential element dx_2 in the direction \mathbf{e}_2 . Note that this situation is met in the dislocation configuration analyzed in [Mori-Tangri,1979]. In this motion, Eq.50 shows that the distortion rate jump $[\![\dot{U}_{22}^p]\!]$ is offset by an opposite jump resulting from the distortion jump $[\![U_{13}^p]\!]$ and the tangential rotation rate $\dot{\Omega}_1$ acting on dx_2 . Thus, surface torsion dynamics derives from the motion in the tangential direction \mathbf{e}_1 of the edge dislocations α_{13} .

The tangential rotation rate of the Darboux frame can be extracted from Eqs.(50,51) in these examples, and in general from Eq.48, as a function of the plastic distortion and distortion rate jumps, provided $[\![\mathbf{U}_p]\!]\cdot\mathbf{n} \neq 0$. Transposing Eq.48 and applying the resulting operators to the normal discontinuity $[\![\mathbf{U}_p]\!]\cdot\mathbf{n}$, we find indeed:

$$([\![\boldsymbol{\alpha} \times (\mathbf{V} - \mathbf{C})]\!] \times \mathbf{n})^t \cdot [\![\mathbf{U}_p]\!]\cdot\mathbf{n} + ([\![\mathbf{U}_p]\!]\cdot\mathbf{n})^2 \dot{\Omega}_t = 0, \quad (53)$$

from which it follows that

$$\dot{\Omega}_t = -([\![\boldsymbol{\alpha} \times (\mathbf{V} - \mathbf{C})]\!] \times \mathbf{n})^t \cdot \frac{[\![\mathbf{U}_p]\!]\cdot\mathbf{n}}{([\![\mathbf{U}_p]\!]\cdot\mathbf{n})^2}. \quad (54)$$

The normal part of the rotation rate, $\dot{\Omega}_n = \dot{s}/R_g \mathbf{n}$, is not used in the theory. Thus, as a consequence of Eq.35, only the evolution of the unit normal \mathbf{n} to the interface can be predicted from Eq.54, whereas the evolution of the tangent vectors $(\mathbf{l}, \boldsymbol{\tau})$ and geodesic curves remains undetermined. Being expressed in terms of tensors and of the normal \mathbf{n} to the interface, $\dot{\Omega}_t$ does not depend on the tangent vectors $(\mathbf{l}, \boldsymbol{\tau})$ or on their orientation

in the tangent plane. The interpretation of Eq.54 is that the normal curvature and torsion dynamics derive from the tangential jump of the relative plastic distortion rate $\boldsymbol{\alpha} \times (\mathbf{V} - \mathbf{C})$, provided that a normal jump of the plastic distortion is existing at all. Such a conclusion is supported by the *in situ TEM* observations reported by [Mori-Tangri,1979] of dislocations gliding along the boundary and featuring line components normal to the boundary in an *Al* bi-crystal. These observations suggest indeed that tangential glide of such dislocations is in direct relation with the curvature of the boundary, which is resolved at a small resolution length scale as a cascade of ledges of about 20Å average height. Finally, we note that a relation similar to Eq.54 can be obtained from Eq.41:

$$\dot{\boldsymbol{\Omega}}_t = -(\llbracket \dot{\mathbf{U}} \rrbracket \times \mathbf{n})^t \cdot \frac{\llbracket \mathbf{U} \rrbracket \cdot \mathbf{n}}{(\llbracket \mathbf{U} \rrbracket \cdot \mathbf{n})^2}. \quad (55)$$

Consequently, the elastic distortion and distortion rate jumps and surface tension effects across the interface must ensure compatibility between Eqs.(54,55).

So far, we have investigated the constraints imposed on the plastic distortion and distortion rate tensors by Burgers vector conservation across curved interfaces moving through the material. This has led to introducing interface rotation as a mechanism for interfacial plasticity able to preserve Burgers vector conservation when a tangential discontinuity of the relative plastic distortion rate is existing. We are now interested in building tools for the analysis of the dynamics of these interfaces, by first investigating constraints on the driving forces and interface mobility relationships that arise from the thermodynamical requirements of positive dissipation.

5 Interface mobility

For convenience, we first recall results on the driving forces on dislocations and their mobility laws in the bulk of the body. The mechanical dissipation D is defined as the difference between the power of applied forces and the rate of change $\dot{\psi}$ of the stored energy:

$$D = \int_{\partial \mathcal{B}} \mathbf{t} \cdot \mathbf{v} dS - \int_{\mathcal{B}} \dot{\psi} dv, \quad (56)$$

where $\mathbf{t} = \mathbf{T} \cdot \mathbf{n}$ and \mathbf{v} are the traction vector and material velocity on the external surface $\partial \mathcal{B}$, of unit normal \mathbf{n} , of the body \mathcal{B} and \mathbf{T} is the (symmetric) Cauchy stress tensor. By using the divergence theorem and balance equations, D is shown to be the volumetric integral:

$$D = \int_{\mathcal{B}} (\mathbf{T} : \dot{\mathbf{U}} - \dot{\psi}) dv. \quad (57)$$

In the linear case, Eq.57 reads as

$$D = \int_{\mathcal{B}} (\mathbf{T} : \dot{\mathbf{U}} - \mathbf{T} : \dot{\mathbf{U}}_e) dv = \int_{\mathcal{B}} \mathbf{T} : \dot{\mathbf{U}}_p dv = \int_{\mathcal{B}} \mathbf{T} : \dot{\boldsymbol{\epsilon}}_p dv, \quad (58)$$

where $\dot{\epsilon}_p = \dot{\mathbf{U}}_p^{sym}$ is the plastic strain rate tensor. Substituting the plastic distortion rate obtained from dislocation motion: $\dot{\mathbf{U}}_p = \boldsymbol{\alpha} \times \mathbf{V}$, D can be cast into the form

$$D = \int_{\mathcal{B}} \mathbf{F} \cdot \mathbf{V} dv, \quad (59)$$

where

$$\mathbf{F} = \mathbf{T} \cdot \boldsymbol{\alpha} : \mathbf{X} \quad (60)$$

is a Peach-Koehler-type driving force on dislocation densities. Whatever the adopted constitutive relationships, D needs to be strictly positive in non-reversible processes such as dislocation motion, and zero in reversible processes such as elastic straining of the body. For example, this condition is satisfied if the constitutive law $\mathbf{F} = B_\alpha \mathbf{V}$ is adopted, with $B_\alpha \geq 0$ as a positive viscous drag parameter.

In the presence of moving surfaces of discontinuity in the body, specific interface dissipation mechanisms add on to bulk mechanisms. Hence, Eq.56 needs to be complemented with a surface integral on I reflecting the difference between the jump of the power of applied forces and the jump of the stored elastic energy across the moving interface. Indeed, the power of external forces is now

$$P = \int_{\partial \mathcal{B}} \mathbf{t} \cdot \mathbf{v} dS + \int_I \llbracket \mathbf{t} \cdot \mathbf{v} \rrbracket dS, \quad (61)$$

and the rate of change of the stored energy Ψ is

$$\frac{d\Psi}{dt} = \int_{\mathcal{B}} \dot{\psi} dS - \int_I \llbracket \psi \rrbracket C_n dS. \quad (62)$$

The first r.h.s. terms in Eqs.(61,62) were accounted for in Eq.56, and the surfacic term in Eq.62 results from the motion of the interface (see for example [Abeyaratne-Knowles,1990]). The dissipation therefore becomes

$$D = \int_{\mathcal{B}} \mathbf{T} : \dot{\mathbf{U}}_p dv + \int_I (\llbracket \mathbf{t} \cdot \mathbf{v} \rrbracket + \llbracket \psi \rrbracket C_n) dS. \quad (63)$$

Such expressions of the mechanical dissipation were used for example by [Cherkaoui et al.,1998] in the context of martensitic transformations and [Berbenni et al.,2013] for boundary migration. Applying the identity: $\llbracket \mathbf{t} \cdot \mathbf{v} \rrbracket = \langle \mathbf{t} \rangle \cdot \llbracket \mathbf{v} \rrbracket + \llbracket \mathbf{t} \rrbracket \cdot \langle \mathbf{v} \rangle$, and noting that $\llbracket \mathbf{t} \rrbracket = 0$ from the continuity of the traction vector across the interface, we obtain

$$\llbracket \mathbf{t} \cdot \mathbf{v} \rrbracket = \langle \mathbf{t} \rangle \cdot \llbracket \mathbf{v} \rrbracket = \langle \mathbf{T} \cdot \mathbf{n} \rangle \cdot \llbracket \mathbf{v} \rrbracket, \quad (64)$$

and using Eq.15:

$$\llbracket \mathbf{t} \cdot \mathbf{v} \rrbracket = - \langle \mathbf{T} \cdot \mathbf{n} \rangle \cdot C_n \llbracket \mathbf{U} \rrbracket \cdot \mathbf{n}, \quad (65)$$

or in component form

$$\llbracket \mathbf{t} \cdot \mathbf{v} \rrbracket = -C_n \langle T_{ij} \rangle n_j \llbracket U_{ik} \rrbracket n_k, \quad (66)$$

which reduces to

$$\llbracket \mathbf{t} \cdot \mathbf{v} \rrbracket = -C_n \langle T_{ij} \rangle \llbracket U_{ij} \rrbracket = -C_n \langle \mathbf{T} \rangle : \llbracket \mathbf{U} \rrbracket. \quad (67)$$

Further, assuming a quadratic potential, homogeneous elasticity and the symmetry relations $C_{ijkl} = C_{jikl} = C_{ijlk} = C_{klij}$ between the elastic moduli, it can be shown that

$$\llbracket \psi \rrbracket = \frac{1}{2}(\mathbf{T}^+ : \mathbf{U}_e^+ - \mathbf{T}^- : \mathbf{U}_e^-) = \langle \mathbf{T} \rangle : \llbracket \mathbf{U}_e \rrbracket. \quad (68)$$

Thus, we obtain from Eqs.(63,67,68):

$$D = \int_{\mathcal{B}} \mathbf{T} : \dot{\mathbf{U}}_p dv - \int_I C_n \langle \mathbf{T} \rangle : (\llbracket \mathbf{U} \rrbracket - \llbracket \mathbf{U}_e \rrbracket) dS, \quad (69)$$

and, using the plastic distortion jump:

$$D = \int_{\mathcal{B}} \mathbf{T} : \dot{\mathbf{U}}_p dv - \int_I C_n \langle \mathbf{T} \rangle : \llbracket \mathbf{U}_p \rrbracket dS. \quad (70)$$

Due to tangential continuity of the plastic distortion along the interface, the inner product in the surface integrand extracts the normal part of the stress tensor, and symmetry of the latter similarly extracts the plastic strain tensor. Thus, Eq.70 is also:

$$D = \int_{\mathcal{B}} \mathbf{T} : \dot{\boldsymbol{\epsilon}}_p dv - \int_I C_n \langle \mathbf{T} \cdot \mathbf{n} \rangle \otimes \mathbf{n} : \llbracket \boldsymbol{\epsilon}_p \rrbracket dS, \quad (71)$$

or

$$D = \int_{\mathcal{B}} \mathbf{T} : \dot{\boldsymbol{\epsilon}}_p dv - \int_I \mathbf{t} \cdot \llbracket \boldsymbol{\epsilon}_p \rrbracket \cdot \mathbf{C} dS \quad (72)$$

if the traction vector \mathbf{t} is used. The volumetric integral was treated above. Along with the dissipation induced by the motion of bulk dislocations, it accounts for the dissipation arising from the motion of interfacial dislocations. In the surface integral, the driving force for the normal motion of the interface is the traction vector, and the relevant conjugated kinematic variable can be identified as

$$\tilde{\mathbf{C}} = -\llbracket \boldsymbol{\epsilon}_p \rrbracket \cdot \mathbf{C} = -C_n \llbracket \boldsymbol{\epsilon}_p \rrbracket \cdot \mathbf{n}. \quad (73)$$

The requirement of non-negativity of the associated dissipation is $\mathbf{t} \cdot \tilde{\mathbf{C}} \geq 0$. The simplest constitutive relationship for the mobility of the interface allowing to satisfy this inequality is the tensorial relation

$$\mathbf{t} = B \tilde{\mathbf{C}} = -B C_n \llbracket \boldsymbol{\epsilon}_p \rrbracket \cdot \mathbf{n}, \quad B \geq 0 \quad (74)$$

where B is a positive viscous drag parameter to which assumptions regarding interface mobility, such as temperature dependence through thermal activation, may be assigned. Eq.74 involves the normal plastic strain discontinuity, a quantity left unconstrained by the Burgers vector conservation requirement across the interface and deriving from tangential glide of the edge dislocations α_{31} and α_{32} . Because their lines are in the interface, these dislocations are not involved in the mechanism leading to interface rotation. Hence, Eq.74 is valid whether the interface is propagating normally to itself or involves a rotation. To illustrate the significance of dissipation positiveness in interface motion, consider dynamic recrystallization and suppose the parent crystal to the left of the interface to be stretched while the embryo to the right is in the natural state, a situation reflected in the inequality $\mathbf{n} \cdot \llbracket \epsilon_p \rrbracket \cdot \mathbf{n} = \llbracket \epsilon_{nn}^p \rrbracket > 0$. Using the projection of Eq.74 along the normal $\mathbf{n} = \mathbf{e}_3$ to the interface, the normal stress is found as

$$T_{33} = -p = -B \llbracket \epsilon_{nn}^p \rrbracket C_n, \quad (75)$$

and positiveness of the dissipation then implies that the interface moves into the parent crystal ($C_n > 0$) if the normal stress is compressive ($p > 0$). Hence, the motion of the interface is such that the material is effectively shortening under pressure, and model materials that would stretch in such conditions are forbidden. Of course, changing the sign of $\llbracket \epsilon_{nn}^p \rrbracket$ would lead to changing the sign of the velocity. In the above illustrative example of a cylindrical interface, Eqs.(52,75) imply

$$T_{33} = B \frac{\llbracket \alpha_{33} V_2^g \rrbracket}{\dot{\Omega}_2} C_3 \quad (76)$$

if $\dot{\Omega}_2 \neq 0$ or equivalently

$$C_n = M \frac{p}{R_n}, \quad (77)$$

if we choose to evidence mobility and the role of the normal curvature. Here, the mobility factor is defined as $M = -\dot{s}/B \llbracket \alpha_{33} V_2^g \rrbracket$. Of course, Eqs.(76,77) do not apply if $\dot{\Omega}_2 = 0$, *i.e.* if the interface propagates normally to itself, in which case its normal velocity is simply given by Eq.75. For a cylindrical interface, Eq.77 is formally similar to Eq.1: the normal velocity of the interface is inversely proportional to its radius of normal curvature and directly proportional to the pressure, which generally comprises an incompatible part deriving from the distribution of dislocations in the body and a compatible one allowing to satisfy equilibrium and the boundary conditions on $\partial\mathcal{B}$. However, the mobility factor M cannot be construed as a simple constitutive parameter as implied by Eq.1. Indeed, in addition to being inversely proportional to the viscous drag parameter, it contains information on the distribution of dislocations, the tangential dislocation velocities and the jumps of plastic distortion rate occurring across the interface. Similar conclusions were recently arrived at from atomistic simulations in [Thomas et al.,2017]. Eq.75 additionally suggests that, along cylindrical interfaces, the interface velocity can be simply

and uniquely determined from the jump of the plastic distortion across the interface and from the traction vector at the interface. Straightforward calculations show that such is also the case when the interface dynamics involves torsion and non-principal normal curvatures.

6 Conclusions

The present paper is first focused on extending the requirements of Burgers vector conservation along interfaces whose propagation involves a rotating Darboux frame. When interfaces propagate normally to themselves (no rotation of the Darboux frame), Burgers vector conservation implies tangential continuity of the plastic distortion and distortion rate tensors [Acharya,2007]. As a consequence, dislocations pertaining to the tangential part of the dislocation density tensor should move with the interface and dislocations belonging to its normal part should not move tangentially along the interface. Nevertheless, such dislocation motion has been observed using *in situ* TEM [Kegg et al.,1973; Mori-Tangri,1979; Momprou et al.,2013] and linked with interface curvature dynamics [Mori-Tangri,1979] or at least with atom shuffling and diffusional processes compatible with a non-trivial interface curvature dynamics [Momprou et al.,2013]. We show here that Burgers vector conservation still holds if the contribution of interface rotation to plasticity is accounted for. Indeed, if the Darboux frame is allowed to rotate, the dislocation-mediated tangential contribution to the relative plastic distortion rate is offset by a contribution arising from the rotation of the interface. This overall balance provides nonlocal dynamic equations for the evolution of the interface normal curvature and torsion radii as functions of the plastic distortion and distortion rate jumps across the interface.

In a second step, the paper explores the constraints on constitutive relationships for interface mobility that arise from positiveness of the dissipation in interface propagation mechanisms. Such thermodynamic constraints provide guidelines for the identification of the conjugated forces and fluxes involved in the normal motion of the interface and the formulation of admissible constitutive laws for the latter. Being determined by jumps of plastic distortion rates supported by volumetric material elements, the interface rotation rate determined above is not directly involved in interface-specific constitutive relationships. Among the latter, the simplest conceivable law involves the normal discontinuity of the plastic strain tensor in a relationship between the traction vector and the normal interface velocity. The proposed constitutive law allows retrieving features of the scalar mobility relationship (1) expected in recovery/recrystallization processes [Humphreys-Hatherly,1995]. Indeed, it is a velocity to driving force relationship. It involves an elastic driving force deriving from the energy stored in the boundary area, and

it features curvature effects, which derive from the dynamics of interface rotation. In addition, it assigns a role to atomic diffusion along the boundary through climb of interfacial edge dislocations, and to external forces applied at the sample boundaries. However, it challenges the constitutive character of the mobility parameter introduced in relation (1) by suggesting its actual dependence on the dislocation density and plastic distortion and distortion rate jumps across the interface.

Phase field methods are an alternative to the present approach based on the mechanics of dislocation fields. The order parameter they introduce allows defining a diffuse boundary and plays the regularizing role assigned to the dislocation density tensor in this work. The time-dependent Ginzburg-Landau formalism is used to derive a kinetics for the order parameter, which results in a relation formally similar to Eq.1. However, it is not a relationship of velocity to driving force and it does not involve the elastic surface energy [Allen-Cahn,1979]. Instead, the interface mobility results from a reaction-diffusion mechanism, and the mean curvature involved in the Allen-Cahn relationship derives from differentiations of the surface free energy with respect to the order parameter. Further, Burgers vector conservation is not naturally enforced, whereas it is instrumental in the present approach, where the interface mobility is essentially consistent with the transport of dislocation densities.

By proposing a three-dimensional physically-based model for the dynamics of curved interfaces, the present analysis opens up an avenue to studying dynamic recrystallization and recovery processes in a thermodynamically / mechanically consistent continuous framework. The next step in this research will be to design consistent algorithms using standard crystal plasticity or the mechanics of dislocation fields [Acharya,2001], and provide solutions of boundary value problems through finite element [Acharya-Roy,2006; Varadhan et al.,2006] or FFT-based spectral approximation methods [Berbenni et al.,2014; Djaka,2015]. For example, nonlinear field dislocation mechanics can be used to determine smooth fields possibly showing discontinuities along propagating surfaces for the dislocation, elastic/plastic distortion and distortion rate tensors, from the solution of boundary value problems. Using the present results, which are fully compatible with this nonlinear framework, this field information allows computing the interface velocity and rotation dynamics. More detailed analyses should involve elastic/plastic rotation jumps as well as the motion of disclinations along the interface. They are postponed for future work.

Acknowledgements

Financial support by the Agence Nationale de la Recherche is gratefully acknowledged (DREAM, ANR-13-BS09-0001-01). This work also benefited from support from the institute INSIS of CNRS and University of Lorraine.

References

- [Abeyaratne-Knowles,1990] R. Abeyaratne and J.K. Knowles, *On the driving traction acting on a surface of strain discontinuity in a continuum*, J. Mech. Phys. Solids, **38**, 345-360 (1990).
- [Acharya,2001] A. Acharya, *A model of crystal plasticity based on the theory of continuously distributed dislocations*, J. Mech. Phys. Solids, **49**, 761-784 (2001).
- [Acharya,2007] A. Acharya, *Jump condition for GND evolution: a connection between grain growth and slip transmission at grain boundaries*, Philos. Mag. **87**, 1349-1359 (2007).
- [Acharya-Roy,2006] A. Acharya, A. Roy, *Size effects and idealized dislocation microstructure at small scales: predictions of a phenomenological model of mesoscopic field dislocation mechanics: I*, J. Mech. Phys. Solids, **54**, 1687-1710 (2006).
- [Allen-Cahn,1979] S.M. Allen, J.W. Cahn, *A microscopic theory for antiphase boundary motion and its application to antiphase domain coarsening*, Acta Metall., **27**, 1085-1095 (1979).
- [Berbenni et al.,2013] S. Berbenni, B. Paliwal and M. Cherkaoui, *A micromechanics-based model for shear-coupled grain boundary migration in bicrystals*, Int. J. Plast. **44**, 68-94 (2013).
- [Berbenni et al.,2014] S. Berbenni, V. Taupin, K.S. Djaka and C. Fressengeas, *A numerical spectral approach for solving elasto-static field dislocation and g-disclination mechanics*, Int. J. Solids Structures **51**, 4157-4175 (2014).
- [Bilby,1955] B.A. Bilby, *Types of dislocation sources*, in: Bristol Conference Report on Defects in Crystalline Solids, The Physical Society, London, 124-133 (1955).
- [Burke-Turnbull,1952] J.E. Burke and D. Turnbull, *Recrystallization and grain growth*, Progress in Metal Physics, **3**, 220-292 (1952).
- [Cahn-Taylor,2004] J.W. Cahn, J.E. Taylor, *A unified approach to motion of grain boundaries, relative tangential translation along grain boundaries, and grain rotation*, Acta Mater. **52**, 4887-4898 (2004).
- [Cahn et al.,2006] J.W. Cahn, Y. Mishin, A. Suzuki, *Coupling grain boundary motion to shear deformation*, Acta Mater., **54**, 4953-4975 (2006).
- [Cartan,1937] E. Cartan, *La théorie des groupes finis et continus et la géométrie différentielle traitées par la méthode du repère mobile*, Gauthier-Villars, Paris (1937).

- [Cherkaoui et al.,1998] M. Cherkaoui, M. Berveiller, H. Sabar, *Micromechanical modeling of martensitic transformation induced plasticity (TRIP) in austenitic single crystals*, Int. J. Plast. **14**, 597-626 (1998).
- [Cordier,2014] P. Cordier, S. Demouchy, B. Beausir, V. Taupin, F. Barou and C. Fressengeas, *Disclinations provide the missing mechanism for deforming olivine-rich rocks in the mantle*, Nature **507**, 51-56 (2014).
- [Csiszár,2011] G. Csiszár, A. Misra, T. Ungár, *Burgers vector types and the dislocation structures in sputter-deposited Cu-Nb multilayers*, Mat. Sci. Eng. A **528**, 6887-6895 (2011).
- [Darboux,1888] G. Darboux, *Leçons sur la théorie générale des surfaces*, Gauthier-Villars, Paris (1888), Chelsea Publ., New-York (1954).
- [Djaka,2015] K.S. Djaka, V. Taupin, S. Berbenni and C. Fressengeas, *A numerical spectral approach to solve the dislocation density transport equation*, Modelling. Simul. Mater. Sci. Eng. **23**, 065008 (2015).
- [Farkas,2006] D. Farkas, A. Froseth, H. Van Swygenhoven, *Grain boundary migration during room temperature deformation of nanocrystalline Ni*, Scripta Materialia **55**, 695-698 (2006).
- [Frank,1950] F.C. Frank, *The resultant content of dislocations in an arbitrary intercrystalline boundary*, in: Symposium on The Plastic Deformation of Crystalline Solids, Mellon Institute, Pittsburgh, (NAVEXOS-P-834), 150-154 (1950).
- [Fressengeas et al.,2012] C. Fressengeas, V. Taupin, M. Upadhyay and L. Capolungo, *Tangential continuity of elastic/plastic curvature and strain at interfaces*, Int. J. Solids Structures, **49**, 2660-2667 (2012).
- [Fressengeas et al.,2014] C. Fressengeas, V. Taupin, L. Capolungo, *Continuous modeling of the structure of symmetric tilt boundaries*, Int. J. Solids Structures, **51**, 1434-1441 (2014).
- [Gianola et al.,2006] D.S. Gianola, S. VanPetegem, M. Legros, S. Brandstetter, H. Van-Swygenhoven, K.J. Hemker, *Stress-assisted discontinuous grain growth and its effect on the deformation behavior of nanocrystalline aluminum thin films*, Acta Mater. **54**, 2253-2263 (2006).
- [Hadamard,1903] J. Hadamard, *Leçons sur la propagation des ondes et les équations de l'hydrodynamique*, Herman, Paris (1903).
- [Humphreys-Hatherly,1995] F.J. Humphreys and M. Hatherly, *Recrystallization and Related Annealing Phenomena*, Pergamon Press, Oxford (1995).

- [Kegg et al.,1973] G.R. Kegg, C. Horton, J.M. Silcock, *Grain boundary dislocations in aluminum bicrystals after high-temperature deformation*, Phil. Mag. **27**, 1041-1055 (1973).
- [Kröner,1981] E. Kröner, *Ergeb. Agnew. Math.* 5. Springer-Verlag. Also: E. Kröner, *Continuum theory of defects*, in: R. Balian, Ed., Les Houches, Session XXXV *Physics of Defects*, North-Holland, Amsterdam, 217-314 (1981).
- [Li,1972] J.C.M. Li, *Disclination model of high angle grain boundaries*, Surface Science **31**, 12-26 (1972).
- [Mach et al.,2010] J. Mach, A.J. Beaudoin, A. Acharya, *Continuity in the plastic strain rate and its influence on texture evolution*, J. Mech. Phys. Solids **58**, 105-128 (2010).
- [Momprou et al.,2009] F. Momprou, D. Caillard and M. Legros, *Grain boundary shear-migration coupling -I. In situ TEM straining experiments in Al polycrystals*, Acta Mater. **57**, 2198-2209, (2009).
- [Momprou et al.,2011] F. Momprou, D. Caillard and M. Legros, *Direct observation and quantification of grain boundary shear-migration coupling in polycrystalline Al*, J. Mater. Sci. **46**, 4308-4313 (2011).
- [Momprou et al.,2013] F. Momprou, M. Legros, A. Boé, M. Coulombier, J.P. Raskin, T. Pardoen, *Inter- and intragranular plasticity mechanisms in ultrafine-grained Al thin films: An in situ TEM study*, Acta Mater. **61**, 205-216 (2013).
- [Mori-Tangri,1979] T. Mori, K. Tangri, *Gliding of Boundary Dislocations on Coincidence Boundaries*, Met. Trans. **10A**, 733-740 (1979).
- [Priester,1979] L. Priester, R.W. Balluffi, *Technique for studying the interaction of lattice dislocations with grain boundaries during plastic deformation*, J. Microsc. Spectrosc. Electr. **4**, 615-622 (1979).
- [Priester,2013] L. Priester, *Grain boundaries From Theory to Engineering*, Springer Series in Materials Science, 172 (2013).
- [Puri,2011] S. Puri, A. Das, A. Acharya, *Mechanical response of multicrystalline thin films in mesoscale field dislocation mechanics*, J. Mech. Phys. Solids **59**, 2400-2417 (2011).
- [Richeton,2011] T. Richeton, G.F. Wang, C. Fressengeas, *Continuity constraints at interfaces and their consequences on the work hardening of metal-matrix composites*, J. Mech. Phys. Solids **59**, 2023-2043 (2011).

- [Roy-Acharya,2005] A. Roy and A. Acharya, *Finite element approximation of field dislocation mechanics*, J. Mech. Phys. Solids **53**, 143-170 (2005).
- [Smoluchowski,1951] R. Smoluchowski, *Theory of grain boundary motion*, Phys. Rev. **83**, 69-70 (1951).
- [Sun et al.,2016] X.Y. Sun, V. Taupin, C. Fressengeas and P. Cordier, *Continuous description of the atomic structure of grain boundaries using dislocation and generalized-disclination density fields*, Int. J. Plast., **77**, 75-89 (2016).
- [Sutton-Balluffi,1995] A.P. Sutton, R.W. Balluffi, *Interfaces in Crystalline Materials*, Clarendon Press, Oxford (1995).
- [Taupin et al.,2014] V. Taupin, L. Capolungo, C. Fressengeas, *Disclination mediated plasticity in shear-coupled boundary migration*, Int. J. Plast. **53**, 179-192 (2014).
- [Taupin et al.,2016] V. Taupin, J. Chevy and C. Fressengeas, *Effects of grain-to-grain interactions on shear strain localization in Al-Cu-Li rolled sheets*, Int. J. Solids Structures, **99**, 71-81 (2016).
- [Thomas et al.,2017] S.L. Thomas, K. Chen, J. Han, P. K. Purohit, D. J. Srolovitz, *Reconciling grain growth and shear-coupled grain boundary migration*, Nature Com., **8**, 1764 (2017).
- [Tucker et al.,2010] G.J. Tucker, J.A. Zimmerman, D.L. McDowell, *Shear deformation kinematics of bicrystalline grain boundaries in atomistic simulations*, Modelling Simul. Mater. Sci. Eng. **18**, 015002 (2010).
- [Varadhan et al.,2006] S. Varadhan, A.J. Beaudoin, A. Acharya and C. Fressengeas, *Dislocation transport using an explicit Galerkin/least-squares formulation*, Modelling Simul. Mater. Sci. Eng. **14**, 1245-1270 (2006).